Rock Mech Rock Eng (2013) 46:635–644
DOI 10.1007/s00603-012-0344-9

ISRM SUGGESTED METHOD

ISRM Suggested Method for Rock Fractures Observations Using a Borehole Digital Optical Televiewer

S. J. Li · Xia-Ting Feng · C. Y. Wang · J. A. Hudson

Published online: 11 December 2012

1 Introduction

Fractures in rock masses are important for the study of a whole range of rock mechanics and rock engineering issues including evaluation of the rock mass geometry, analysis of the Excavation Damaged Zone (EDZ), understanding the rock mass behaviour and response to excavation, numerical analyses, and reinforcement/support design.

A digital borehole camera records a continuous, magnetically orientated digital 360° colour image of the borehole wall, making it possible to directly observe lithological changes in the rock mass and its contained fractures (Paillet et al. 1990; Pusch 1998). Fractures display sinusoidal curves on the flattened image, enabling the strike and dip of the fractures to be determined directly from the images orientated to North (Kamewada et al. 1989; Wang et al. 2002; Williams and Johnson 2004). The technology has been widely applied in geological exploration, especially in petroleum (Maddox 1998; Tague 1999; Palmer and Sparks 1991), mining (Gochioco et al. 2002; Deltombe and Schepers 2000), Glacier (Engelhardt et al. 1978), geotechnical and environmental engineering (Lau et al. 1987; Miyakawa et al. 2000; Lahti 2004; Cunningham 2004; Cunningham et al. 2004; Schepers et al. 2001; Roberson and Hubbard 2010; Uchita and Harada 1993; Li et al. 2012a). It has also been used to observe crack development and fracture evolution around underground excavations, contributing to the establishment of the EDZ characteristics (Li et al. 2012a, b; Yuji 1983).

There are two main types of digital borehole camera used: the first is a digital optical televiewer, such as the OPTV (Optical Televiewer), OTV (Optical Televiewer) and OBI-40 (Slimhole Optical Televiewer) (Williams and Johnson 2004; Lahti 2004; Cunningham 2004; Cunningham et al. 2004; Schepers et al. 2001; Roberson and Hubbard 2010); the other is a digital panoramic borehole camera, such as the DIPS (Borehole Image Processing System) and DPBCS (Digital Panoramic Borehole Camera System) (Wang et al. 2002; Wang and Law 2005; Williams and Johnson 2004; Uchita and Harada 1993; Li et al. 2012a). The main parameters of these two kinds of camera are listed in Table 1.

The first digital camera was developed as a stand-alone system in 1987 (Williams and Johnson 2004). Since then the tool has gradually become a standard tool. Although there are different types of digital camera system, the basic principle, components and operations of these test systems are almost the same. Thus, this Suggested Method describes the observation of fractures in a rock mass and the identification of EDZ. The apparatus and operating procedure are presented together with the possible ways of reporting the results. The recommendations are supported by case example data.

2 Scope

This Suggested Method is intended to directly observe fractures in a rock mass using a digital optical borehole

Please send any written comments on this ISRM Suggested Method to Prof. Resat Ulusay, President of the ISRM Commission on Testing Methods, Hacettepe University, Department of Geological Engineering, 06800 Beytepe, Ankara, Turkey.

S. J. Li · X.-T. Feng (✉) · C. Y. Wang
State Key Laboratory of Geomechanics and Geotechnical Engineering, Institute of Rock and Soil Mechanics, Chinese Academy of Sciences, Wuhan 430071, Hubei, China
e-mail: xtfeng@whrsm.ac.cn; xia.ting.feng@gmail.com

J. A. Hudson
Department of Earth Science and Engineering, Imperial College, London, SW7 2AZ, UK

Table 1 Technical specifications of representative borehole digital optical camera systems

Name	CCD pixels	Precision (mm)		Probe (mm)		Test velocity (m/min)	Colour (bits)	Borehole diameter (mm)
		Horizontal	Vertical	Diameter	Length			
OPTV	768 × 494	0.331	1.000	52	1,630	2.5	24	56–180
				61				
OBI 40	795 × 596	0.331	0.375	40	1,700	1.5	16/24	42–180
BIPS	795 × 596	0.331	0.250	42	1,540	0.9	16/24	55–180
				50				
DPBCS	795 × 596	0.325	0.160	45	350	1.5	16/24	48–91
				72	485			76–180

camera through pre-drilled boreholes, with characteristics of the fractures being surveyed in both air and clear fluid-filled boreholes.

Based on the comparison of fractures observed at different times (Li et al. 2012a, b), the evolution characteristics of fractures, including initiation, propagation and closure, occurring in the rock mass are obtainable.

According to in situ observation of the evolution characteristics of fractures subject to excavation or rheological effect (Li et al. 2012a, b), the EDZ in the rock mass is identified based on the new fractures observable via the precision of the digital optical borehole camera.

This Suggested Method can also be adopted to detect possible stress induced damages in the borehole, and hence help to estimate in situ stress orientation.

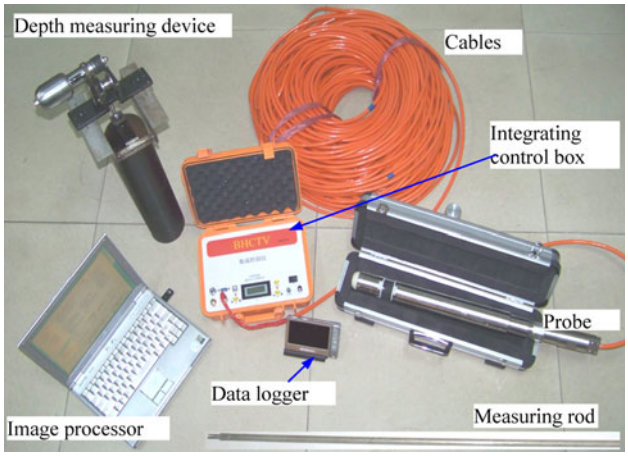

Fig. 1 The basic components of a typical borehole digital optical camera system. Note the photo of the components may change in case of the different borehole digital optical camera system

3 Apparatus

3.1 Basic Components

The apparatus related to this in situ observation of rock mass fractures mainly consists of the probe, depth measuring device, integrating control box, data logger (portable media player or computer), cables, and alternative measuring rods for horizontal or inclined boreholes, as shown in Fig. 1.

3.2 Probe

The probe is the core component for the capture of borehole wall images. Probes in different diameter sizes are available as an option from 40 to 72 mm, and the diameter for test borehole should be in the range 42–180 mm, less than 110 mm for better quality of borehole wall images resulting in more effective identification of fractures and EDZ.

The key component of the digital optical borehole camera is a conical mirror installed in the probe as the reflector. The functions of the conical mirror are as follows.

1. Reflecting the light emitted from the probe light source used to illuminate the borehole wall.
2. Reflecting the borehole wall information into the probe for the camera records.
3. Note that the radius of both the top and the bottom surfaces of the conical mirror determine the radius of the panoramic image. Also, the deformation mode of the conical mirror determines the changing manner of the borehole wall information in the panoramic image (Wang et al. 2002; Wang and Law 2005).

Fractures evident in the panoramic image are the projections of the fractures on the conical mirror. The borehole wall in the panoramic image is represented as a ring, in which the inner circle is the upper end of the borehole wall and the outer circle is the lower end. The position of a point on the borehole wall as displayed on the ring is related to the azimuth of this point. In the panoramic image, horizontal and vertical fractures display concentric circle and radial lines, respectively, whereas inclined fractures are like conic curves. Figure 2a–e indicate the changing nature

of the eastward fracture in the panoramic image. Points A, C and M, shown in Fig. 2, are located on a fracture. Points B and D are located in the west and east directions, respectively. As shown in Fig. 2a, the underside of the conical mirror is over the highest point A of the fracture; point A and parts of the fracture around it are in the outer circle, which appears as a conical curve. Point A is the cusp. Figure 2b shows that point B is in the same position as point A. The conical mirror is in the middle of the fracture, and point C is to the south of the fracture with an orientation of 180°, as shown in Fig. 2c. Figure 2d indicates that the topside of the conical mirror will be over the point D in the borehole wall. As presented in the panoramic image, point D is moving from the outer circle to the edge of the inner circle and ready to leave the ring. Also, as shown in Fig. 2e, the underside of the conical mirror is over the lowest point of the fracture. Point M is at an orientation of 90°, the fracture around which is displayed as a conical shape, and point M is the cusp.

3.3 Depth Measuring Device

There are two ways to test the depth of the probe in the borehole. One method is to record the length of each measuring rod manually, another method is to test the depth using depth measuring equipment installed at the borehole outlet. The data are displayed on the borehole wall images in real time and stored together with the image file. The depth measuring device mainly consists of the test wheel, photoelectric corner encoder and acquisition board. The test wheel is rotated by the friction between the rod/cable and wheel, and the depth measuring device records the depth in electronic pulse counting mode through a photoelectric corner encoder. The distance of the rod/cable moving through the test wheel is converted into an electronic signal by an acquisition board. Then, the depth is calculable according to the rotation angles of the test wheel and the number of electronic pulses. The information is transferred to the interface board in the integrating control box and superimposed on panoramic images.

3.4 Integrating Control Box and Data Logger

The integrating control box is the power supply for the whole testing system, which controls the collection, input and output of the panoramic video signal and depth pulse signal. It is also used to connect the data logger and real-time image capture interface. The data logger is used for the storage of the borehole wall images and depth information in two different ways. One approach is through obtaining the video file in AVI format using video acquisition equipment and transferring the file into a personal computer for image process. In this case, portable media player is available, it can also be used as a video monitor. Another approach is connecting the personal computer through an interface in the integrating control box and obtaining the flattened borehole wall images directly in a specialized software platform.

3.5 Cables and Measuring Rods

The boreholes for this Suggested Method can be divided into three types namely vertical, horizontal and inclined boreholes. Cables are essential for signal transmission. For the in situ measurements of vertical or sub-vertical (inclination angle 75°–90°) boreholes, some special carrying cables should be required to undertake the weight of probe and groundwater pressure in some deep boreholes. Whereas measuring rods should be taken for horizontal and inclined borehole with the inclination angle 0°–75°.

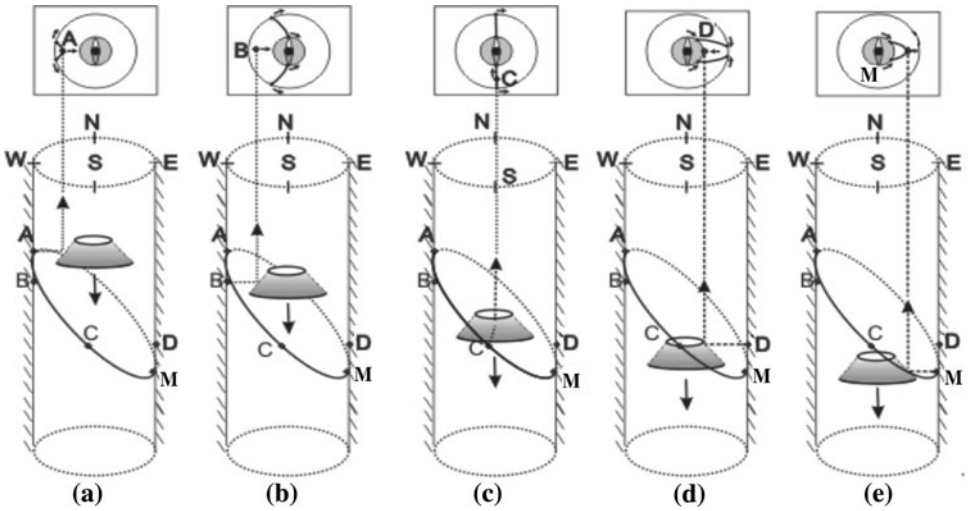

Fig. 2 The changing appearance of the fracture in the panoramic image

The installation and connection diagram for all the components of a borehole digital optical camera system are shown in Fig. 3.

3.6 Drilling Equipment

In order to conduct in situ borehole measurements of rock mass fractures, appropriate drilling equipment is required for the borehole drilling whatever with core or not. Any equipment capable of producing a stable hole to the required test depth and diameter may be used. Commonly, the drilling rig should have the properties of low weight, easy handling and vertical and inclined borehole double use.

In general, both percussive and rotative drilling methods are acceptable. However, the borehole wall should be well flushed by clean water when percussive drilling adopted. It is suggested that lining would be required in some circumstances. For instance, when the rock top is under a soil/decomposed rock layer.

4 Procedure

4.1 Layout of Boreholes

The layout of boreholes depends on the test goals concerned. Commonly, there are two approaches for borehole layout.

1. When the test objective is the understanding of rock mass structure, boreholes can be configured directly to the rock mass in real time at any position and angle, as shown in Fig. 4a.
2. When the test goal is to investigate the fracture evolution or zonal disintegration of rock mass (Qian et al. 2009), the boreholes should be pre-drilled before excavation of tunnels (Fig. 4b), so as to observe the entire process of fracture initiation, propagation and closure before, during and after tunnel construction.

In an underground construction project, taken as the example and as shown in Fig. 4b, borehole is drilled from the pre-excavated underground tunnels to the test object. In order to fully reveal the characteristics of fractures and their evolutionary processes, the borehole diameter for fracture observation is suggested to be in the range 42–110 mm in view of the performance of the CCD digital camera and obtainable quality of borehole images. The length (S) and dip (θ) of the borehole are determined by the distance and spatial location between the test site and the object to be observed. Nevertheless, it is important that the length of borehole must pass through the rock mass around the test object. For example, the borehole needs to pass through the side wall of a test tunnel to be excavated.

4.2 Drilling and Inspection

Percussive and rotative drilling methods are acceptable as mentioned above. It is recommended that rock cores should be obtained during rotative drilling, and so diamond bit drilling should be adopted. Synthetic comparison of rock cores and images of borehole wall will lead to better understanding of geological conditions and rock mass fractures. The choices of borehole length and orientation are made taking into account the position of the object to be tested.

It is recommended that the drilling rig should be kept steady with the drilling speed less than 600 r/min, so that the borehole wall can be maintained smooth and straight without ridges or steps from the tunnels to the bottom of the borehole, as far as possible to make it easy for the probe's movement.

On the basis of rock cores, geological recording should be carried out during drilling, and the positions, orientations and apertures of geological discontinuities observed in the borehole should be estimated.

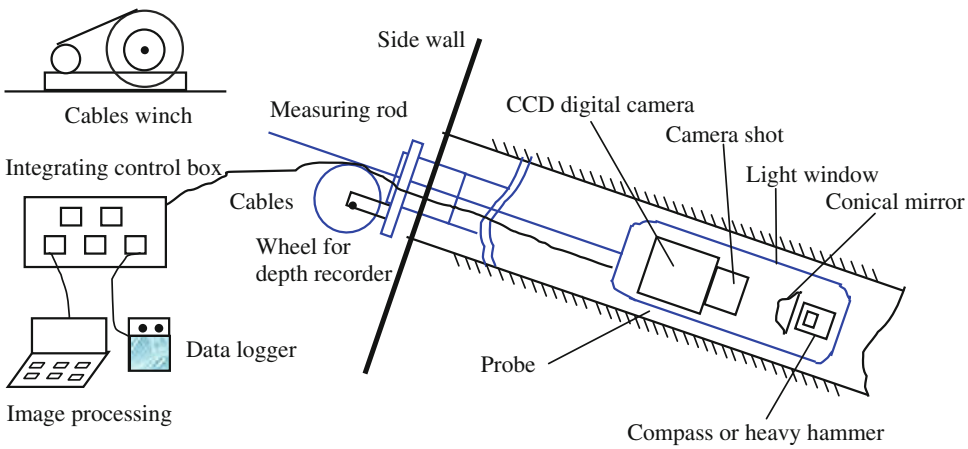

Fig. 3 Sketch of the installation and connection system for the borehole digital optical camera in situ testing system

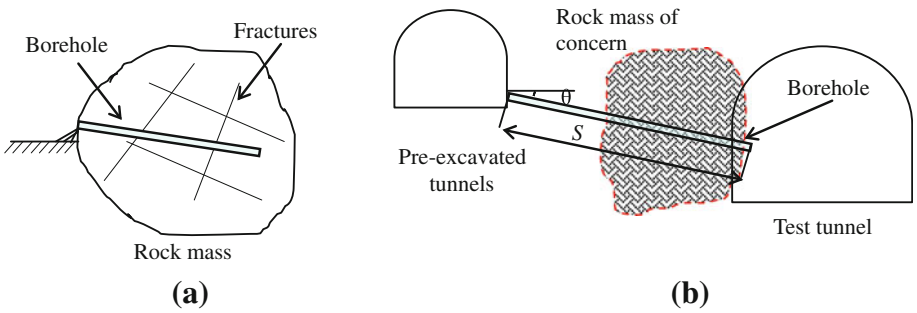

Fig. 4 Examples of borehole layouts for measurements of rock mass fractures. **a** Borehole configured directly into the rock mass in real time at any position and angle. **b** Borehole layouts determined by the pre-installed method

All of the boreholes to be observed should be flushed to remove debris or fractured rocks after drilling. It is also strongly recommended that the boreholes should be rinsed using clean water. However, in case of some severely weak or fractured stratum, drillers use bentonite or casing to prevent the collapse of the hole. The borehole wall can not be effectively observed by an optical camera. In this case, clean water should be used to flush some portions which the test mainly concerned and also the casing should be pulled out. If the borehole collapses seriously under this condition leading to the probe incapable of running through, drill pipes may be used to cope with the debris or fractured rocks. If all the remedial measures can not work, the borehole has to be scrapped and a new one should be drilled close to this position.

4.3 Observation of Rock Mass Fractures

(a) Analyse the borehole drill records and associated histograms. If rotative drilling method is employed and rock cores are available, preliminarily analyse the characteristics of the stratum, geological defects and groundwater.
(b) Flatten the test site to place all the monitoring facilities and relevant subsidiary equipment, connect water pump and water pipe, clean test boreholes to remove dust, mud and drilling waste slag.
(c) Set and connect the test equipment, install and fix the depth measuring device near the borehole orifice, install the push rod through the depth measuring wheel and adjust it to the centre of the borehole orifice.
(d) Choose a suitable probe with an appropriate diameter (according to the borehole diameter), put the probe into the borehole orifice and connect with the push rod tightly.
(e) Connect the power cable, panorama probe signal cable, depth pulse signal cable, video signal cable and computer interface successively.
(f) Connect the power, press the light switch and the zero depth switch.
(g) Turn on the data logging and start to monitor and record depth and videos.
(h) Let the probe run in the borehole slowly from top to bottom under the action of measuring rods or cables (length of each rod is 1.0 or 1.5 m), note that the advancing speed of the probe should be uniform and less than 1.5 m/min to obtain clear images.
(i) According to observations of the borehole from the camera, write down the depth of probe advance in the borehole manually every 1.0 or 1.5 m and record the depth on the data logging monitoring screen at the same time. In brief, describe factors such as groundwater, rock mass integrity and fractures from the monitoring video in real time.
(j) When the probe reaches the bottom of the borehole, the test is completed. Turn off the camera and the control box power, and save the video files. Disassemble the push rods and pull the probe out of the borehole slowly.
(k) Check the state of the probe, clean and pack it in a dedicated box, and leave the test site after checking other equipment such as depth measuring device, integrating control box, computer, pump, and so on.

Based on the captured digital images stored in video file format, the digital image processing will be carried out in specially developed software so that facture images in a flattened mode and virtual core can be obtained. Further analysis involves rock lithology, fracture distribution, position, occurrence and width, evolution characteristics when the objective is to characterize the EDZ compared to construction progress.

4.4 Identification of EDZ

At present, there are several conceptions on the EDZ definition according to the project type, testing methods and research goals. Among them, the common content of EDZ is the region where the rock properties and conditions have changed due to fracturing, stress redistribution and desaturation (Egger 1989; Martino and Chandler 2004). Many indirect methods have been taken to determine the EDZ of rock mass by measuring the decrease of acoustic velocity, change of hydraulic transport properties, etc. It indicates

that direct observation of fracture changes is also an effective method which can reflect the permanent change of rock mass. The EDZ can be identified by directly observing fracture modifications via the precision of the borehole digital optical camera. The maximum resolution of the current borehole digital optical camera is 0.1–0.2 mm, while it will be continuously improved as the development of the CCD digital camera technology.

For this purpose, a series of flattened images of borehole wall observed in different time by borehole digital optical camera are needed. Evolutionary characteristics of width, length and occurrence of new and pre-existing fractures are to be analyzed. The EDZ of rock mass is identified by comparison of these flattened images observed in different time. The EDZ is determined to be the zone where new fractures are detected.

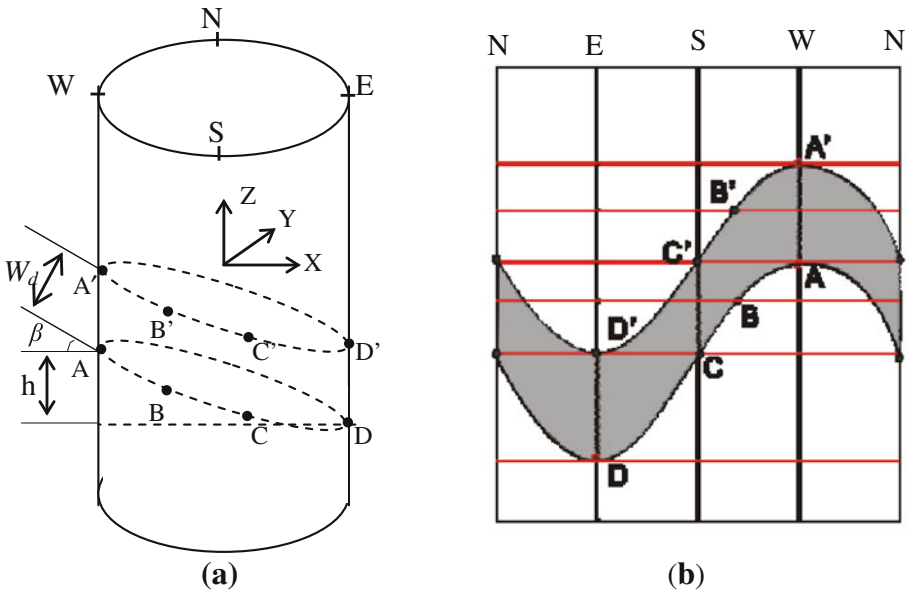

Fig. 5 Sketch diagram of the calculation co-ordinates of fracture occurrence

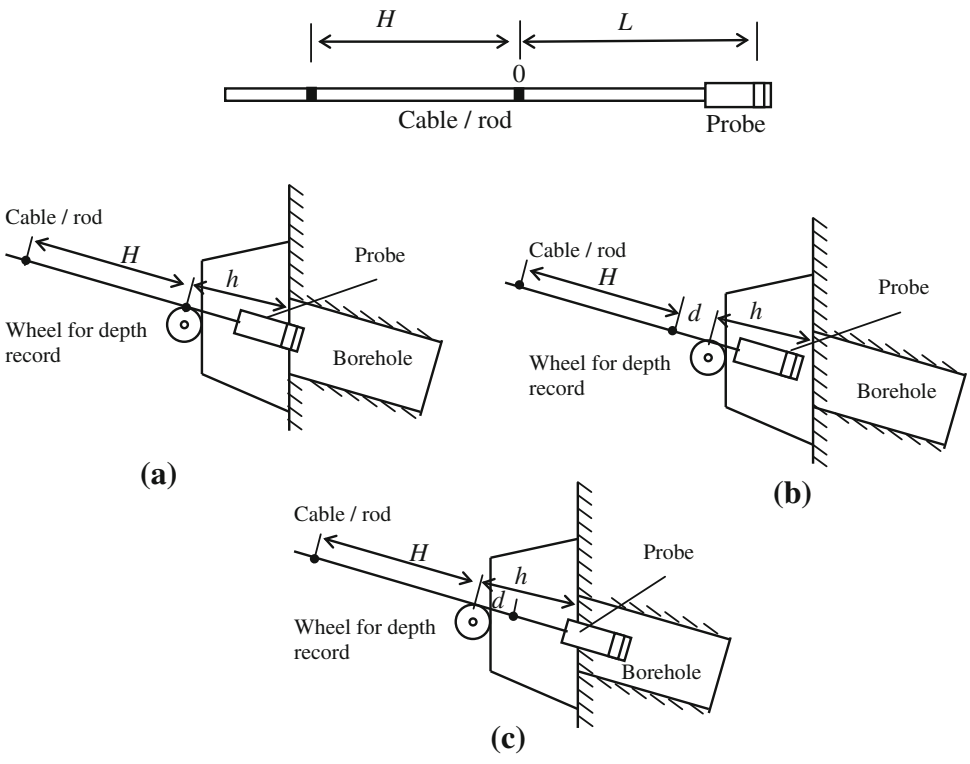

Fig. 6 The relation between the recorded depth by cumulative number of cable or measuring rods and the actual depth (**a** $L = h$, **b** $L > h$, **c** $L < h$)

5 Calculations

5.1 Calculation of the Occurrence and Width of the Observed Rock Mass Fractures

When a complete fracture is at an angle to the borehole, the projection is displayed as a sinusoidal curve on the flattened image, as shown in Fig. 5.

It is assumed that the Z axis is the central axis of the borehole with the positive direction vertically upwards, and the plane fixed by axes X and Y is perpendicular to axis Z with the positive direction to the East and North, respectively (Fig. 5a). The calculation of the orientation of the rock mass fracture is described as follows.

Taking three non-collinear points A, C and D on a fracture shown in the flattened pattern, two vectors $\bar{V}_1$ and $\bar{V}_2$ in this plane can be obtained and described as:

$$\bar{V}_1 = \overline{AC},\ \bar{V}_2 = \overline{AD} \tag{1}$$

The normal vector of this plane can be described as:

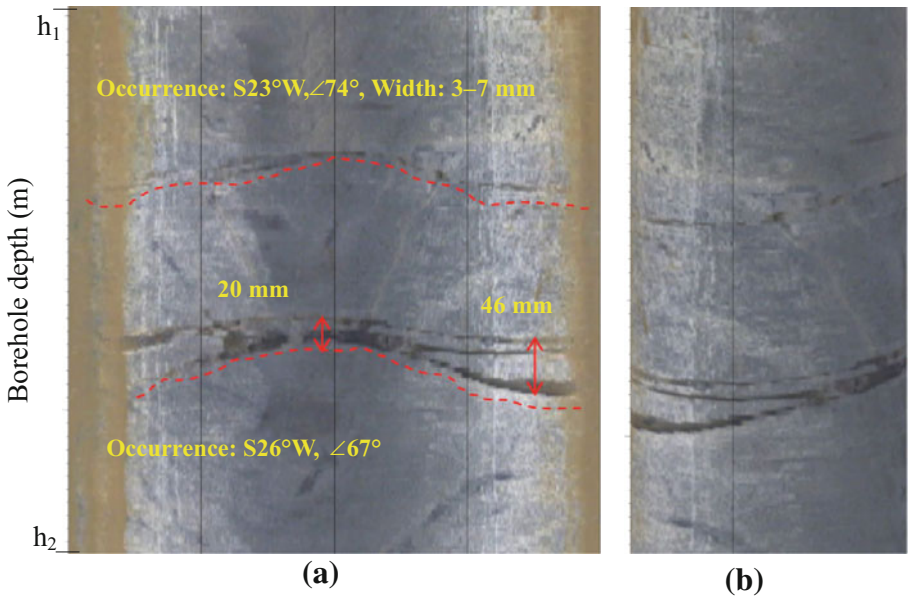

Fig. 7 Images of the borehole wall shown in **a** flattened pattern, **b** virtual core. (The *dashed lines* indicate the traces of the fractures; the *arrows* indicate the widths of fractures)

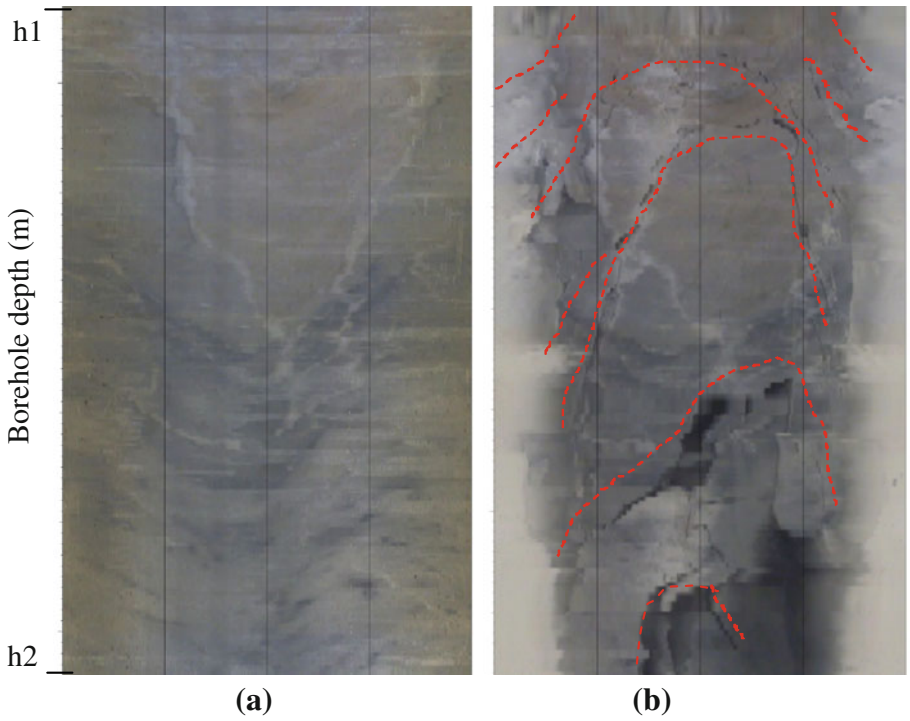

Fig. 8 Comparison of borehole wall images for fracture evolution studies: **a** original rock mass, **b** new fractures that have appeared due to time effect or excavation of rock mass. (*Dashed lines* are the traces of the fractures)

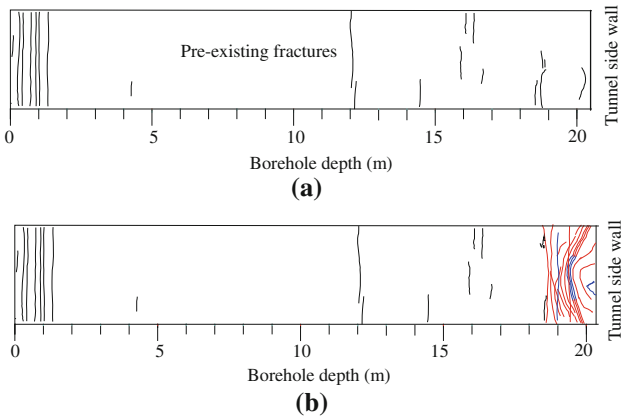

Fig. 9 Sketch plan of fracture distribution and evolution measured at different time of excavation steps: **a** pre-existing fractures, **b** abundant new fractures at another time due to time effect or excavation disturbance

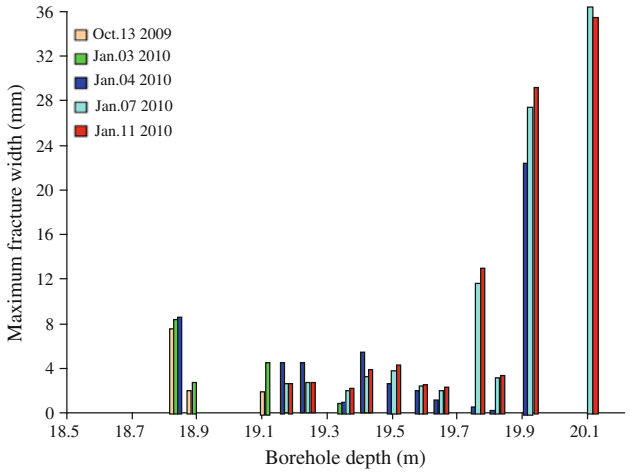

Fig. 10 Change of fracture width over time, as observed at different times

$$\overline{N} = \bar{V}_1 \times \bar{V}_2 \tag{2}$$

In order to represent the unit normal vector, Eq. (2) can be transformed as:

$$\overline{N_u} = \overline{N} / \left\| \overline{N} \right\| \tag{3}$$

If the Z-component of the unit normal vector is less than zero, the opposite vector $\overline{N_0} = \{X_0, Y_0, Z_0\}$ will be expressed as:

$$\overline{N_0} = -\overline{N_u} \tag{4}$$

So, the dip angle β of the fracture can be calculated as:

$$\beta = \cos^{-1} Z_0 \tag{5}$$

It can also be expressed as:

$$\beta = \tan^{-1}(h/d) \tag{6}$$

where h is the vertical distance of points A and D, d is the diameter of test borehole.

Assuming that $\overline{N_p} = \{X_p, Y_p\}$ is the projection of the unit normal vector $\overline{N_0}$ on the XY plane, then the dip azimuth α of the fracture can be calculated as:

$$\alpha = \begin{cases} 90^\circ - \tan^{-1} Y_p/X_p & \text{when } X_p > 0 \\ 90^\circ & \text{when } X_p = 0 \text{ and } Y_p > 0 \\ 270^\circ - \tan^{-1} Y_p/X_p & \text{when } X_p < 0 \\ 270^\circ & \text{when } X_p = 0 \text{ and } Y_p < 0 \end{cases} \tag{7}$$

According to the relationship between dip azimuth and orientation, the orientation of the fracture can be calculated as:

$$\theta = \begin{cases} \alpha + 90^\circ & \text{when } \alpha < 90^\circ \\ \alpha - 90^\circ & \text{when } \alpha \geq 90^\circ \end{cases} \tag{8}$$

The width of the fracture can be obtained by measuring the spatial distance of any relevant two points A and A' located on opposite sides of the fracture, which is described as:

$$W_d = \sqrt{(X_A - X_{A\prime})^2 + (Y_A - Y_{A\prime})^2 + (Z_A - Z_{A\prime})^2} \cdot \cos\beta \tag{9}$$

5.2 Calculation of the Ratio Coefficient Between the Actual Depth and the Test Depth

Each image records a test depth (S_t), which is determined by a depth measuring wheel through an electronic pulse counting mode. Due to the friction of the measuring wheel and the sliding of the push rod, S_t is a little different from the actual probe depth (S_p) in the borehole. Therefore, it is necessary to obtain the ratio coefficient R between actual depth and test depth which is an important factor in the digital image processing software. Based on the proportional coefficient, the test depths of each segmental image can be calibrated.

As shown in Fig. 6, it is assumed that the distance between every two points of cable depth marks or length of each measuring rod is H, the distance from the zero point to the transparent window of the probe is L, the distance from the depth testing wheel and cable or testing rod tangent point to the orifice of the borehole is h, and the advancing distance of the probe is recorded as S.

If $L = h$, then $S_p = S$.

If $L > h$, then $S_p = S - (h + d + L)$.

If $L < h$, then $S_p = S + (L + d - h)$.

The ratio coefficient R between the actual depth and the test depth is expressed as:

$$R = \frac{S_p^i - S_p^{i-1}}{S_t^i - S_t^{i-1}} \tag{10}$$

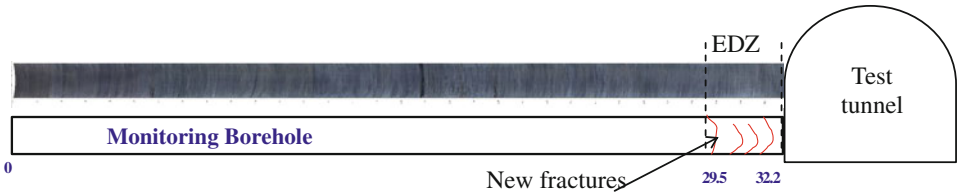

Fig. 11 Schematic diagram of the EDZ assessment based on the distribution of new fractures

6 Reporting of Results

The report should include the following general information.

(a) A description of the test site and lithology.
(b) Description of the condition of groundwater in boreholes if there is groundwater in it, the depth of groundwater from the surface in borehole is needed to be given.
(c) Description of the lining located at some portion of the borehole when weak or fractured stratum exists.
(d) The location, diameter, length, direction and dip angle of the boreholes.
(e) The testing equipment, diameter of probe, cable depth marks and length of unique measuring rod.
(f) Testing date, total testing time of each borehole and depth records of borehole segments.

The report should also include the following detailed information of rock mass fractures:

(a) 360° RGB orientated images of the borehole wall for the whole length, shown in the flattened pattern and virtual core, as shown in Fig. 7.
(b) Statistics of the calculation results for fracture occurrence, location, width and properties.
(c) Description of construction scheme, excavation progress and geological sketching if EDZ identification is to be analyzed.
(d) Comparison of the borehole wall images with fracture changes due to the time effect or construction disturbance, including the evolution of fracture initiation, propagation and closure, as shown in Fig. 8.
(e) Sketch plan of fracture evolution and distribution displayed on flattened sides measured at different time or excavation steps, as shown in Fig. 9.
(f) Evolutionary characteristics of fracture width at different test times or excavation stage, as shown in Fig. 10.
(g) Identification of the EDZ according to the method previously mentioned in procedure. For the observation of the rock mass around tunnels, the results show the determination of the EDZ with new fractures being observed at the maximum resolution 0.1–0.2 mm of a borehole digital optical camera, as shown in Fig. 11.

References

Cunningham KJ (2004) Application of ground-penetrating radar, digital optical borehole images, and cores for characterization of porosity hydraulic conductivity and paleokarst in the Biscayne aquifer, southeastern Florida, USA. J Appl Geophys 55:61–76

Cunningham KJ, Carlson JI, Hurley NF (2004) New method for quantification of vuggy porosity from digital optical borehole images as applied to the karstic Pleistocene limestone of the Biscayne aquifer, southeastern Florida. J Appl Geophys 55(1–2):77–90

Deltombe JL, Schepers R (2000) Combined processing of BHTV travel time and amplitude images. In: Proceedings from the seventh international symposium on minerals and geotechnical logging, Golden, Colorado, October 24–26, pp 1–13

Egger P (1989) Study of excavation induced rock damage at the Grimsel underground rock laboratory. Nucl Eng Ng Des 116:11–19

Engelhardt HF, Harrison WD, Kamb B (1978) Basal sliding and conditions at the glacier bed as revealed by bore-hole photography. J Glaciol 20(84):469–508

Gochioco LM, Magill C, Marks F (2002) The borehole camera: an investigative geophysical tool applied to engineering, environmental and mining challenges. Lead Edge Soc Explor Geophys 21(5):474–477

Kamewada S, Endo T, Kokubu H, Nishigaki Y (1989) The device and features of BIP system [A]. In: The 21st symposium on rock mechanics proceedings, committee on rock mechanics [C]. [sl.], Japanese Society of Civil Engineers, pp 196–200

Lahti M (2004) Digital borehole imaging of the boreholes KR24 upper part and PH1 at Olkiluoto, Posiva Oy. Working Report 2004-28, p 21

Lau JSO, Auger LF, Bisson JG (1987) Subsurface fracture surveys using a borehole television camera and acoustic televiewer. Can Geotech J 24:499–508

Li SJ, Feng X-T, Li ZH, Chen BR, Zhang CQ, Zhou H (2012a) In situ monitoring of rockburst nucleation and evolution in the deeply buried tunnels of Jinping II hydropower station. Eng Geol 137–138:85–96

Li SJ, Feng XT, Li ZH, Zhang CQ, Chen BR (2012b) Evolution of fractures in the excavation damaged zone of a deeply buried tunnel during TBM construction. Int J Rock Mech Min Sci 55(10):125–138

Maddox SD (1998) Application of downhole video technology to multilateral well completions. J Petrol Tech 50(6):34–36

Martino JB, Chandler NA (2004) Excavation-induced damage studies at the underground research laboratory. Int J Rock Mech Min Sci 41(8):1413–1416

Miyakawa K, Tanaka K, Hirata Y, Kanauchi M (2000) Detection of hydraulic pathways in fractured rock masses and estimation of conductivity by a newly developed TV equipped flowmeter. Eng Geol 56(1–2):19–27

Paillet FL, Barton C, Luthi S, Rambow F, Zemanek JR (1990) Borehole imaging and its application in well logging-an overview. Borehole Imaging, Society of Professional Well Log Analysts, Inc., 6001 Gulf Freeway, Suite C129, Reprint Series, Houston, Texas, pp 3–23

Palmer ID, Sparks DP (1991) Measurement of induced fractures by downhole television camera in coalbeds of the Black Warrior basin. J Petrol Tech 43(3):270–275

Pusch R (1998) Practical visualization of rock structure. Eng Geol 49(3–4):231–236

Qian QH, Zhou XP, Yang HQ et al (2009) Zonal disintegration of surrounding rock mass around the diversion tunnels in Jinping II Hydropower Station, Southwestern China. Theor Appl Fract Mec 51:129–138

Roberson S, Hubbard B (2010) Application of borehole optical televiewing to investigating the 3-D structure of glaciers: implications for the formation of longitudinal debris ridges, midre Lovénbreen, Svalbard. J Glaciol 56(195):143–156

Schepers R, Rafat G, Gelbke C, Lehmann B (2001) Application of borehole logging, core imaging and tomography to geotechnical exploration. Int J Rock Mech Min Sci 38(6):867–876

Tague JR (1999) Downhole video optimizes scale removal program. Petrol Eng Int 72(7):27–32

Uchita Y, Harada T (1993) Behavior of discontinuous rock during large underground cavern excavation. In: Proceedings of the International Symposium on Assessment and Prevention of Failure Phenomena in Rock Engineering, Istanbul, Turkey, pp 807–816

Wang CY, Law KT (2005) Review of borehole camera technology. Chin J Rock Mech Engng 24(19):3440–3448 (in Chinese)

Wang CY, Law KT, Sheng Q, Ge XR (2002) Borehole camera technology and its application in the Three Gorges project. In: Proceedings of the 55th Canadian geotechnical and 3rd joint IAH-CNC and CGS groundwater specialty conferences, Niagara Falls, Ontario, pp 601–608

Williams JH, Johnson CD (2004) Acoustic and optical borehole-wall imaging for fractured-rock aquifer studies. J Appl Geophys 55(1–2):151–159

Yuji K (1983) Observation of crack development around an underground rock chamber by borehole television system. Rock Mech and Rock Eng 16(2):133–142